ORIGINAL ARTICLE

Exogenous bone morphogenetic protein-7 reduces hepatic fibrosis in *Schistosoma japonicum*-infected mice *via* transforming growth factor-β/Smad signaling

Bo-Lin Chen, Jie Peng, Qing-Fu Li, Min Yang, Yuan Wang, Wei Chen

Bo-Lin Chen, Jie Peng, Qing-Fu Li, Yuan Wang, Department of Gastroenterology, Xiangya Hospital, Central South University, Changsha 410008, Hunan Province, China
Min Yang, Department of Respiration, Hunan Children's Hospital, Changsha 410011, Hunan Province, China
Wei Chen, Department of Gastroenterology, Changsha Central Hospital, Changsha 410004, Hunan Province, China
Author contributions: Chen BL designed the research, performed the majority of the experiments and wrote the manuscript; Peng J supervised the research; Yang M was involved in revising the manuscript; Li QF, Wang Y and Chen W helped perform the research and participated in data analysis.
Correspondence to: Dr. Jie Peng, Department of Gastroenterology, Xiangya Hospital, Central South University, Changsha 410008, Hunan Province, China. pengjie2@medmail.com.cn
Telephone: +86-731-84327321 Fax: +86-731-84327321

Abstract
AIM: To investigate the antifibrotic effects of bone morphogenetic protein-7 (BMP-7) on *Schistosoma japonicum* (*S. japonicum*)-induced hepatic fibrosis in BALB/C mice.

METHODS: Sixty BALB/C mice were randomly divided into three groups, including a control group (group A, *n* = 20), model group (group B, *n* = 20) and BMP-7 treated group (group C, *n* = 20). The mice in group B and group C were abdominally infected with *S. japonicum* cercariae to induce a schistosomal hepatic fibrosis model. The mice in group C were administered human recombinant BMP-7. Liver samples were extracted from mice sacrificed at 9 and 15 wk after modeling. Hepatic histopathological changes were assessed using Masson's staining. Transforming growth factor-beta 1 (TGF-β1), alpha-smooth muscle actin (α-SMA), phosphorylated Smad2/3 (pSmad2/3) and Smad7 protein levels and localization were measured by Western blotting and immunohistochemistry, respectively, and their mRNA expressions were detected by reverse transcription-polymerase chain reaction (RT-PCR).

RESULTS: The schistosomal hepatic fibrosis mouse model was successfully established, as the livers of mice in group B and group C showed varying degrees of typical schistosomal hepatopathologic changes such as egg granuloma and collagen deposition. The degree of collagen deposition in group C was higher than that in group A (week 9: 22.95 ± 6.66 *vs* 2.02 ± 0.76; week 15: 12.84 ± 4.36 *vs* 1.74 ± 0.80; *P* < 0.05), but significantly lower than that in group B (week 9: 22.95 ± 6.66 *vs* 34.43 ± 6.96; week 15: 12.84 ± 4.36 *vs* 18.90 ± 5.07; *P* < 0.05) at both time points. According to immunohistochemistry data, the expressions of α-SMA, TGF-β1 and pSmad2/3 protein in group C were higher than those in group A (α-SMA: week 9: 21.24 ± 5.73 *vs* 0.33 ± 0.20; week 15: 12.42 ± 4.88 *vs* 0.34 ± 0.27; TGF-β1: week 9: 37.00 ± 13.74 *vs* 3.73 ± 2.14; week 15: 16.71 ± 9.80 *vs* 3.08 ± 2.35; pSmad2/3: week 9: 12.92 ± 4.81 *vs* 0.83 ± 0.48; week 15: 7.87 ± 4.09 *vs* 0.90 ± 0.45; *P* < 0.05), but significantly lower than those in group B (α-SMA: week 9: 21.24 ± 5.73 *vs* 34.39 ± 5.74; week 15: 12.42 ± 4.88 *vs* 25.90 ± 7.01; TGF-β1: week 9: 37.00 ± 13.74 *vs* 55.66 ± 14.88; week 15: 16.71 ± 9.80 *vs* 37.10 ± 12.51; pSmad2/3: week 9: 12.92 ± 4.81 *vs* 19.41 ± 6.87; week 15: 7.87 ± 4.09 *vs* 13.00 ± 4.98; *P* < 0.05) at both time points; the expression of Smad7 protein in group B was higher than that in group A and group C at week 9 (8.46 ± 3.95 *vs* 1.00 ± 0.40 and 8.46 ± 3.95 *vs* 0.77 ± 0.42; *P* < 0.05), while there were no differences in Smad7 expression between the three groups at week 15 (1.09 ± 0.38 *vs* 0.97 ± 0.42 *vs* 0.89 ± 0.39; *P* > 0.05). Although minor discrepancies were observed, the results of RT-PCR and Western blotting were mainly consistent

with the immunohistochemical results.

CONCLUSION: Exogenous BMP-7 significantly decreased the degree of hepatic fibrosis in both the acute and chronic stages of hepato-schistosomiasis, and the regulatory mechanism may involve the TGF-β/Smad signaling pathway.

INTRODUCTION

Schistosomiasis japonica, a chronic and debilitating disease caused by the trematode *Schistosoma japonicum* (*S. japonicum*), is one of the major public health problems in China and other tropical countries such as the Philippines and Indonesia. It seriously impacts the health of residents within endemic areas as well as social and economic development[1-3]. Human immune response to schistosome eggs deposited in the liver and the granulomatous inflammation they evoke are the initial factors of hepato-schistosomiasis, while the subsequent hepatic fibrosis represents a wound-healing response to previous liver damage[4-8]. The primary cell type involved in schistosomal hepatic fibrosis is the hepatic stellate cell (HSC); HSCs are activated in response to inflammatory injury and converted from vitamin A-storing cells into myofibroblasts-like cells, characterized by the expression of alpha-smooth muscle actin (α-SMA), the secretion of excessive collagens and other extracellular matrix components, and the production of various pro-fibrosis cytokines such as transforming growth factor-beta (TGF-β)[9-11]. TGF-β not only maintains the progressive activation of myofibroblasts, but also activates other silent HSCs[12,13]. This positive feedback cascade reaction always causes continuous schistosomal hepatic fibrosis even when timely and effective anti-helminthic treatment has been given. In addition, praziquantel resistance has become common because of a long term dependence on this single anthelmintic[14,15]. As etiological therapy alone is not enough to treat hepatic fibrosis, finding other strategies that can block the activation of HSCs and suppress the progression of collagen deposition is important. Considering the dominant role of the cytokine system in hepatic fibrosis, research on cytokine regulators (antagonist or promoter) has become a new focus and has very promising value.

Among the numerous cytokines and growth factors that are involved in hepatic fibrosis, TGF-β, especially TGF-β1, is an acknowledged critical fibrogenic stimulus to HSCs[16,17]. TGF-β performs its functional role mostly *via* the TGF-β/Smad signaling pathway, which is implicated in a wide range of physiological and pathological events, including embryogenesis, inflammation and fibrosis. In this pathway, phosphorylated Smad2/3 (pSmad2/3) proteins act as pivotal downstream effectors of TGF-β which convey signals from TGF-β receptors to the nucleus, while Smad7 seems to be antagonistic to TGF-β as a negative feedback mediator[18-21]. Bone morphogenetic protein-7 (BMP-7), a member of the TGF-β superfamily, has been studied extensively due to its essential roles during morphogen formation and cell differentiation[22,23]. Recently, its therapeutic potential in the regulation of fibrosis was recognized based on the counteractive effect of BMP-7 against the TGF-β/Smad signaling pathways. For instance, Zeisberg *et al*[24] demonstrated the Smad-dependent reversal of TGF-β1-induced epithelial-to-mesenchymal transition (EMT) by BMP-7 to renal tubular epithelial cells, while EMT is recognized as an important event in fibrogenesis. Moreover, varying degrees of inhibition of thioacetamide- and CCL4-induced liver fibrosis by BMP-7 has been respectively observed in recent research[25]. These limited findings led us to hypothesize that BMP-7 may have a similar effect on schistosomal hepatic fibrosis. Therefore, in the current study, we set TGF-β1 and Smads as our intervention targets to investigate the potential therapeutic effect of BMP-7 in a mouse model of schistosomal hepatic fibrosis.

MATERIALS AND METHODS

Animals and parasite

Six-week-old SPF BALB/C female mice, weighing 12-16 g, were obtained from the Experimental Animal Center, Central South University, Changsha, China. All animal experiments were performed under the control of the Animal Care Committee of Central South University in accordance with the Guidelines on Animal Experiments in Central South University. *Oncomelania hupensis* harboring *S. japonicum* cercariae were purchased from the Institute of Schistosomiasis Control Center (Yueyang, Hunan, China) and the vitality of cercariae was confirmed by microscopy.

Animal treatment

Sixty BALB/C mice were randomly divided into three groups, including a control group (group A), model group (group B) and BMP-7 treated group (group C) (*n* = 20 in each group). All animals were maintained under specific pathogen-free conditions, kept at 20 ℃-25 ℃ in a 12-h light/12-h dark cycle and had free access to standard laboratory water and chow. The mice in group B and group C were percutaneously infected with *S. japonicum* by placing a coverslip carrying 15 ± 1 cercariae in non-chlorine water on their abdomen for 30 min. The mice in group A were treated with non-chlorine water containing no cercariae. Six weeks after infection, the initial phase of hepatic schistosomiasis where, according to our previous

studies[26], schistosome eggs reached the liver, the mice in group C were administered recombinant human BMP-7 (Peprotech, United States, Catalog Number: 120-03), 300 pg/g intraperitoneally, every other day for a period of four weeks. At 9 wk and 15 wk after infection, which are the extreme and stationary phases of schistosomal hepatic fibrosis according to our previous studies[26], 10 mice from each group were randomly selected and sacrificed. Liver tissues were obtained and divided into two parts: the left lobes were fixed in a 4% paraformaldehyde solution for 12 h and the remainder was preserved at -80 ℃ until use.

Histological examination

After a graded alcohol series, dehydration and xylene treatment, the liver specimens were embedded in paraffin blocks and cut into 5-μm thick sections. The degree of collagen deposition was assessed using Masson's staining according to standard procedures. A pathologist who was blinded to the research design checked all the sections and described the pathological changes mainly concerning hepatic fibrosis. In addition, a medical color image analysis system (Image-Pro Plus 6.0) was used to scan and sum the collagen deposition areas then calculate the percentage of collagen, a relative objective index to assess the degree of hepatic fibrosis, expressed as the ratio of the fibrotic area to the whole area. The field examined at 100× magnification contained at least a granuloma, portal area, or a centrilobular vein, and the results are presented as the mean of ten different fields in each section.

Immunohistochemistry

Immunohistochemical staining was performed with an HRP-Polymer anti-Mouse/Rabbit IHC Kit (MAIXIN-BIO, China, Catalog Number: KIT-5020). The sections were dewaxed, dehydrated, washed in phosphate-buffered saline (PBS, 0.01 mol/L, pH 7.2) 3 × 5 min, heated at 100 ℃ in a microwave oven 6 × 2 min, incubated in 3% H_2O_2 in deionized water for 10 min to block endogenous peroxides activity, and washed 3 × 5 min with PBS. The sections were then incubated overnight at 4 ℃ with primary antibodies (rabbit TGF-β1 antibody, sc-146, Santa Cruz Biotechnology, Inc., 1:500; goat p-Smad2/3 antibody, sc-11769, Santa Cruz Biotechnology, Inc., 1:300; mouse Smad7 antibody, sc-365846, Santa Cruz Biotechnology, Inc., 1:300; rabbit α-SMA antibody, ab5694, Abcam, Inc., 1:400). After washing 3 × 5 min with PBS, the appropriate HRP-polymer anti-mouse/rabbit immunoglobulin G (IgG) was added to the sections and incubated at 37 ℃ for 20 min. The sections were then washed 3 × 5 min with PBS, and the color was developed with DAB for 3-5 min. The nuclei were lightly counterstained with hematoxylin. Negative controls were incubated with PBS without the primary antibody. The integral optical density (IOD) of the target protein was measured with Image-Pro Plus 6.0, and the result was determined as the sum of five different fields (one in the center and four in the periphery) of each section. IOD was defined as the sum of the optical densities of all the positive pixels in the image, which represents the quantity of the targeted protein.

Reverse transcription-polymerase chain reaction

Total RNA was extracted from preserved liver tissue with TRIZOL Reagent (Invitrogen, United States) then reverse-transcribed into cDNA by polymerase chain reaction (PCR). Mix Reagent kits (Fermentas, Canada) were used according to the manufacturer's protocol. The housekeeping gene, glyceraldehyde-3-phosphate dehydrogenase (GAPDH), was used as an internal control to calculate relative quantification of target gene expression. The primer sequences were as follows: TGF-β1 (168 bp) forward 5'-AGGGCTACCATGCCAACTTC-3' and reverse 5'-CCACGTAGTAGACGATGGGC-3'; Smad2 (148 bp) forward 5'-CTGTGACGCATGGAAGGTCT-3' and reverse 5'-CCACGTAGTAGACGATGGGC-3'; Smad3 (135 bp) forward 5'-CAGCGAGTTGGGGGAGACATT-3' and reverse 5'-TGTAAGTTCCACGGCTGCAT-3'; Smad7 (230 bp) forward 5'-GCACTCGGTGCTCAAGAAAC-3' and reverse 5'-CCGAGGAATGCCTGAGATCC-3'; α-SMA (300 bp) forward 5'-AAGAGCATCCGACACTGCTG-3' and reverse 5'-AATAGCCACGCTCAGTCAGG-3'; GAPDH (132 bp) forward 5'-AACTTTGGCATTGTGGAAGG-3' and reverse 5'-GGATGCAGGGATGATGTTCT-3'. In the RT step, a 20 μL reaction volume contained the following components: 1 μL RNA sample (1 μg/μL), 1 μL Oligo (dT) (10 pmol/μL), 10 μL DEPC-water, 4 μL 5 × buffer, 2 μL dNTP mixture (10 mmol/L), 1 μL RNase inhibitor (10 U/μL) and 1 μL ReverTra Ace. The reaction was performed at 25 ℃ for 5 min, followed by 42 ℃ for 60 min, 70 ℃ for 5 min, and 4 ℃ for 5 min. In the PCR step, a 25 μL reaction volume contained the following components: 12.5 μL 2 × Master Mix, 10.5 μL nuclease-free water, 1 μL primer, and 1 μL cDNA. The PCR protocol was as follows: denaturation at 94 ℃ for 3 min; 35 cycles of denaturation at 94 ℃ for 30 s, annealing at 59 ℃ (TGF-β1, Smad2, Smad3 and GAPDH)/58 ℃ (Smad7 and α-SMA) for 30 s, and elongation at 72 ℃ for 45 s; and final elongation at 72 ℃ for 5 min. The amplified products were separated by electrophoresis on 1.5% agarose gels (volume: 8 μL samples plus 2 μL buffer; voltage: 100 V), visualized with ethidium bromide staining and photographed using an ultraviolet imaging system (Kodak, United States). We used gel analysis software (Gel-Pro 4.0) to scan and calculate the IOD of strips. The relative mRNA expression of the target gene was represented as the ratio of target gene IOD and GAPDH IOD.

Western blotting

Liver tissues (0.5 g) were homogenized on ice in 1 mL lysis buffer prepared from a Total Protein Extraction kit (ProMab, United States) for about 20 min and then ultrasonicated for 3 × 3 s. The homogenates were centrifuged at 9000 × *g* for 10 min at 4 ℃ and the supernatants were then extracted to obtain the gel sample by mixing it with sampling buffer. Following heat denaturation at 100 ℃ for 3 min, the samples (20 μg protein each lane) were separated by sodium dodecyl sulfate-polyacrylamide

gel electrophoresis in running buffer and subsequently transferred to nitrocellulose membrane (Pierce, United States) in precooling transfer buffer at 300 mA constant current for 70 min. Non-specific binding site sealing was performed by incubating in PBS containing 5% non-fat milk for 2 h at room temperature. The primary antibodies (rabbit TGF-β1 antibody, sc-146, Santa Cruz Biotechnology, Inc., 1:400; goat p-Smad2/3 antibody, sc-11769, Santa Cruz Biotechnology, Inc., 1:500; mouse Smad7 antibody, sc-365846, Santa Cruz Biotechnology, Inc., 1:800; rabbit α-SMA antibody, ab5694, Abcam, Inc., 1:500; mouse GAPDH antibody, SC-365062, Santa Cruz Biotechnology, Inc., 1:800) were incubated with the membrane overnight at 4 ℃. After being washed 5 × 4 min with PBS-Tween 20 (PBST), the secondary antibody (goat anti-rabbit IgG HRP for TGF-β1 and α-SMA, 1:40 000; rabbit anti-goat IgG HRP for p-Smad2/3, 1:40 000; goat anti-mouse IgG HRP for Smad7 and GAPDH 1:80 000) was incubated with these membranes for 1 h at room temperature. After being washed 5 × 4 min with PBST, enhanced chemiluminescence detection of the target protein was performed. The film was scanned and the image was analyzed with Gel-Pro 4.0. The relative expression of target protein was represented by the ratio of target protein IOD and GAPDH IOD.

Statistical analysis

Statistical analysis was performed using SPSS 13.0 software. Comparisons between groups were performed using one-way analysis of variance (homogeneity of variance: S-N-K; heterogeneity of variance: Dunnett's T3). Comparisons between time points were performed using independent-samples t test. P values less than 0.05 were considered statistically significant.

RESULTS

Schistosomal hepatopathology

Typical schistosomal hepatopathological characteristics include mainly egg granuloma and collagen deposition and were observed using Masson's staining in group B and group C at both time points (Figure 1C-F), while group A showed normal hepatocyte morphology (Figure 1A and B). At week 9, in group B, a dense mass of collagen fibers surrounded the egg granulomas, and spread to the space around them, or extended to neighboring lobules (Figure 1C); in group C, there were still numerous collagen fibers around the granulomas, but these were fewer (Figure 1E). At week 15, compared to week 9, a reduction in collagen deposition in group B was observed (Figure 1D), while there were only a few collagen fibers wrapped around disintegrated granulomas in group C (Figure 1F). Data of the percentage of collagen fibers in the different groups and at the two time points are expressed as the mean ± SD and are shown in Figure 1G.

Expression of TGF-β1, α-SMA, pSmad2/3 and Smad7 (immunohistochemistry)

Wispy traces of TGF-β1 positive staining were sparsely distributed in sections of group A (Figure 2A and D). At week 9, in group B, densely TGF-β1-stained cells which could be distinguished by their yellow, brownish-yellow or snuff color surrounded and infiltrated the granulomas, and accumulated in fibrotic lesions or stretched along the fibrous septum (Figure 2B); in group C, the quantity and intensity of positive traces were reduced compared to group B (Figure 2C) ($P < 0.05$). At week 15, in group B, there were still some TGF-β1-stained cells wrapped around the fibrotic granulomas or scattered around them (Figure 2E); however, only a few dispersed yellow traces were seen in group C (Figure 2F) ($P < 0.05$). The variation in α-SMA and pSmad2/3 expressions between the time points and groups were similar to TGF-β1, although discrepancies were observed (Figure 2G-L and Figure 3A-F). It is worth mentioning that pSmad2/3 was mainly located in the nuclei not only in fibrocytes and inflammatory cells, but also in normal hepatocytes (Figure 3A-F). The expression of Smad7 in the three groups was different, and was only observed at week 9 in group B. At this point, brownish-yellow traces were distributed around the granulomas and scattered in the surrounding normal hepatic tissue (Figure 3H), but no positive staining was observed in other cells (Figure 3G and I-L). Figure 2M and N, Figure 3M and N show the IODs of each target protein in the different groups and time points. These results are expressed as IOD ($\times 10^2$ or $\times 10^3$) and as the mean ± SD.

Expression of TGF-β1, α-SMA, pSmad2/3 and Smad7 mRNA (RT-PCR) and protein (Western blotting)

The experimental data on target mRNAs (RT-PCR) and proteins (Western blotting) were all roughly consistent with the immunohistochemical results (Figures 4 and 5). In summary, the expressions of TGF-β1, pSmad2/3 and α-SMA mRNA and protein in group C were higher than or similar to those in group A, but significantly decreased compared to group B at both time points. With regard to the expressions of Smad7 mRNA and protein, there were no significant differences between group A and group C at both time points or group B at week 15, but they were all lower than those in group B at week 9. All data are shown in Figures 6 and 7.

DISCUSSION

The molecular components and regulatory mechanism of the TGF-β/Smad signaling pathway are more or less diverse under different pathologic processes and environmental conditions[27-30]. During acute liver injury, especially in toxipathic hepatitis, the principal components and the canonical progression of this signaling are as follows: catalytically active TGF-β type I receptor phosphorylates Smad2 and the highly similar protein Smad3 to create their phosphorylated (p) isoforms, then TGF-β promotes collagen synthesis in activated HSCs via pSmad2/3 pathways[31]. In the recovery stage of acute liver injury, to avoid excessive collagen deposition, TGF-β also initiates the expression of antagonistic Smad7 which functions in a negative-feedback loop to reduce the fibro-

Week 9

Week 15
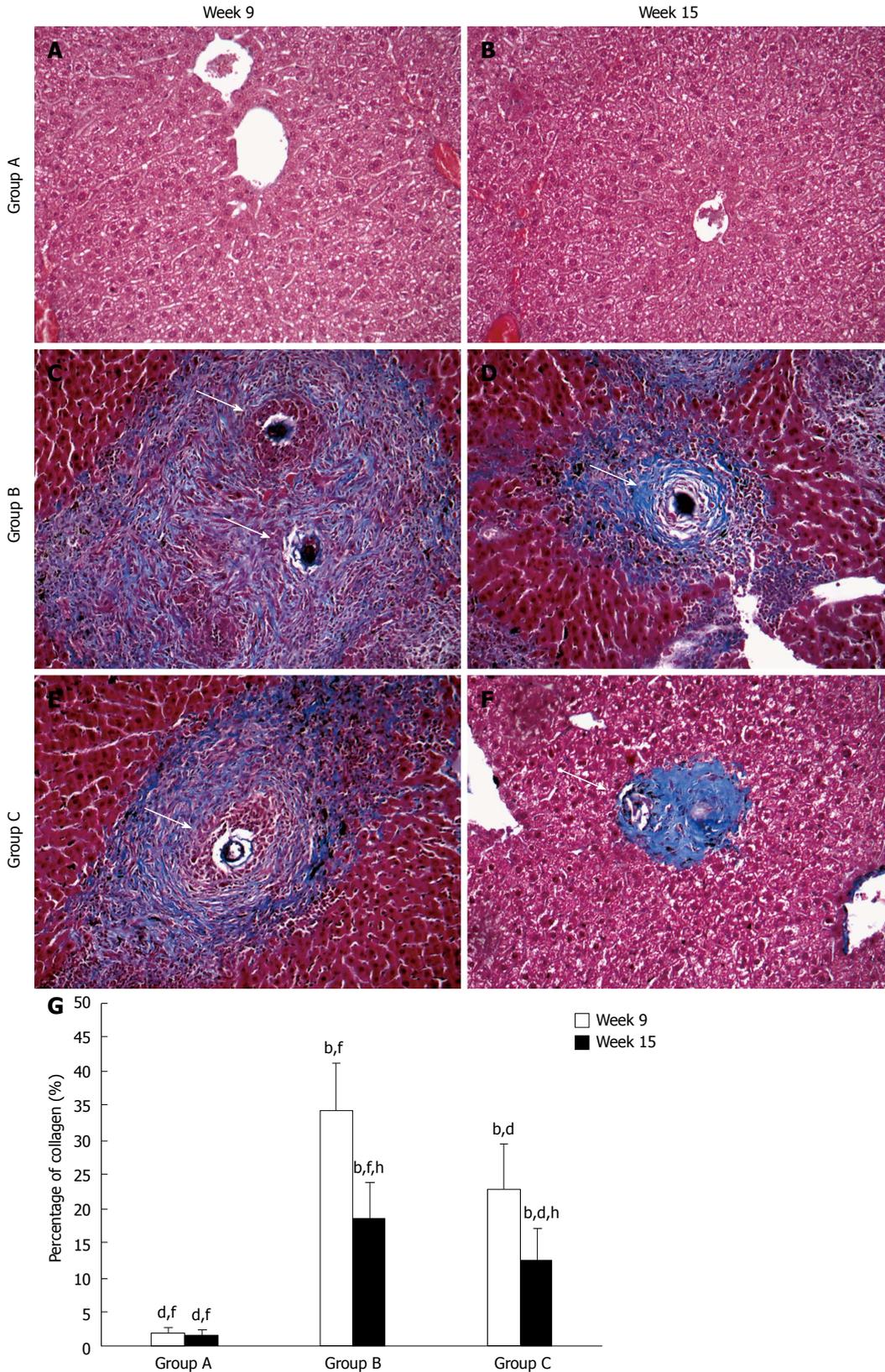
Figure 1 Representative images of schistosomal hepatic fibrosis in the groups over time. Collagen fibers are stained blue and arrows show egg granulomas. Original magnification 100×. Histogram shows the percentage of collagen which represented the degree of hepatic fibrosis. [b]$P < 0.01$ *vs* group A; [d]$P < 0.01$ *vs* group B; [f]$P < 0.01$ *vs* group C; [h]$P < 0.01$ *vs* week 9.

genic strength of the signal[32,33]. However, the negative regulation of TGF-β/Smad signaling is insufficient and

transitory; when liver injury and fibrosis enter the chronic phase, the induction of Smad7 gradually ceases, while
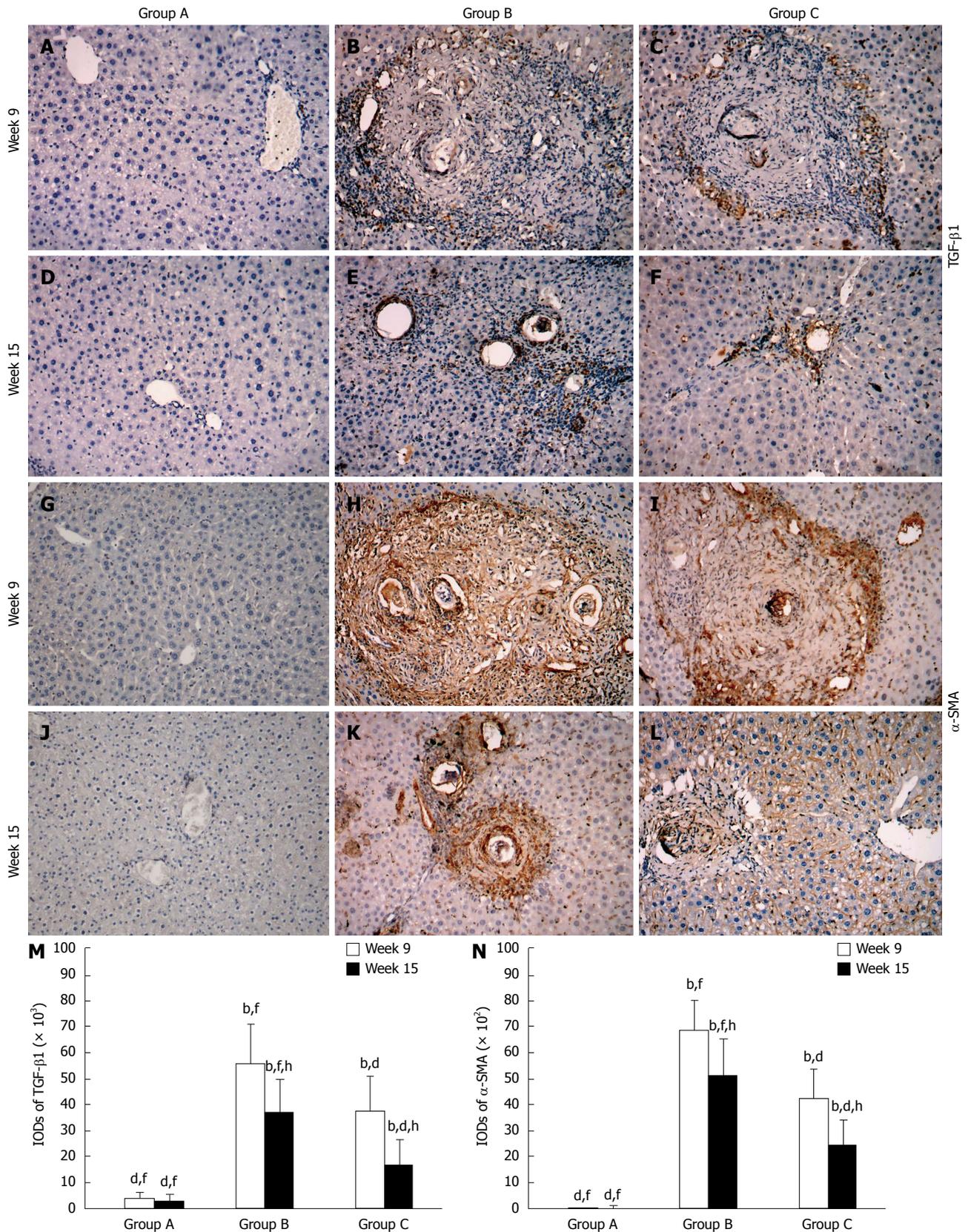
Figure 2 Representative images of immunostaining for transforming growth factor-beta 1 and alpha-smooth muscle actin in the groups over time. Target protein positive staining is yellow, brownish-yellow or snuff. Original magnification 100×. Histogram shows integral optical densities of target proteins. TGF-β1: Transforming growth factor-beta 1; α-SMA: Alpha-smooth muscle actin; IOD: Integral optical density. [b]$P < 0.01$ *vs* group A; [d]$P < 0.01$ *vs* group B; [f]$P < 0.01$ *vs* group C; [h]$P < 0.01$ *vs* week 9.

other promotive factors continue to work[34]. That is why

an appropriate exogenous cytokine regulator is so attrac-
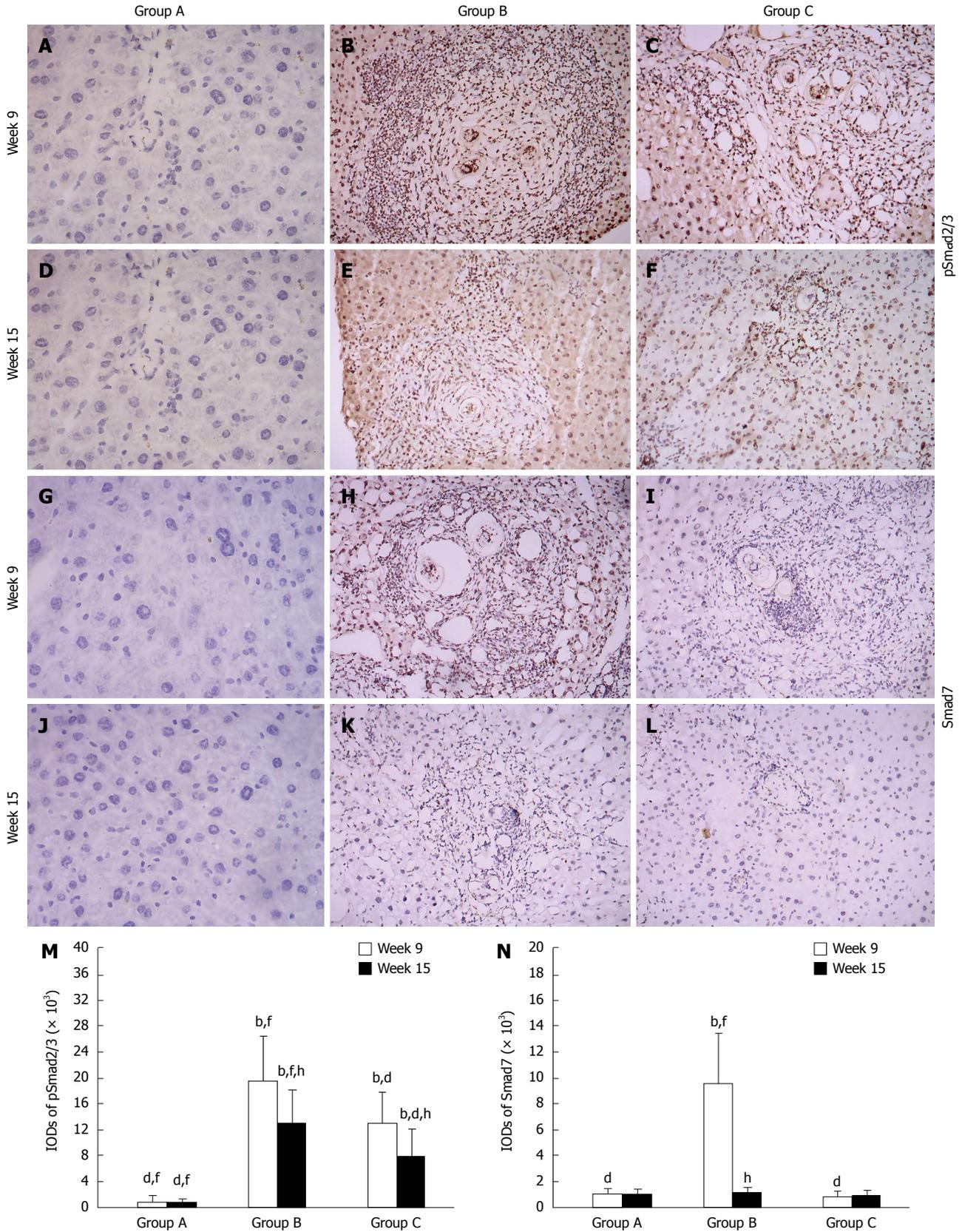
Figure 3 Representative images of immunostaining for pSmad2/3 and Smad7 in the groups over time. Target protein positive staining is yellow or brownish-yellow. Original magnification 100×. Histogram shows integral optical densities of target proteins. [b]$P < 0.01$ *vs* group A; [d]$P < 0.01$ *vs* group B; [f]$P < 0.01$ *vs* group C; [h]$P < 0.01$ *vs* week 9. IOD: Integral optical density.

tive due to its potential therapeutic effect in blocking or reversing hepatic fibrosis. Although BMP-7 belongs to
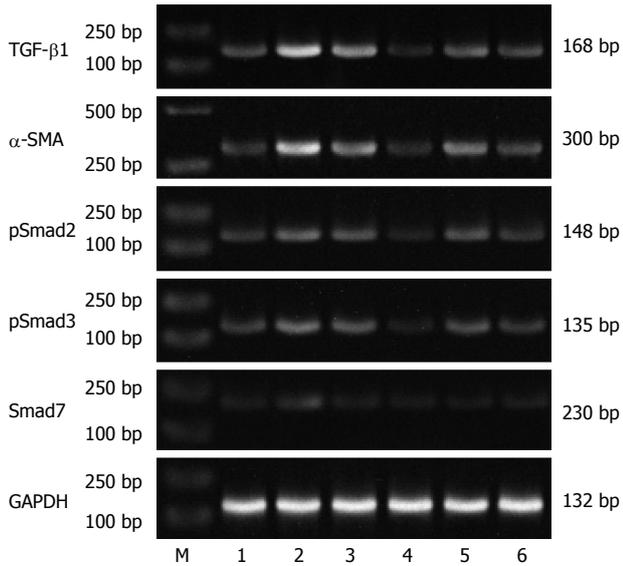
Figure 4 Representative electrophoretic bands of transforming factor-beta 1, alpha-smooth muscle actin, pSmad2, pSmad3 and Smad7 mRNA (reverse transcription-polymerase chain reaction). Numbers 1-3 represent group A, B and C, respectively, at 9 wk; Numbers 4-6 represent group A, B and C, respectively, at 15 wk. The 132 bp glyceraldehyde-3-phosphate dehydrogenase (GAPDH) mRNA fragment was used as an internal control. M: Marker; TGF-β1: Transforming growth factor-beta 1; α-SMA: Alpha-smooth muscle actin.
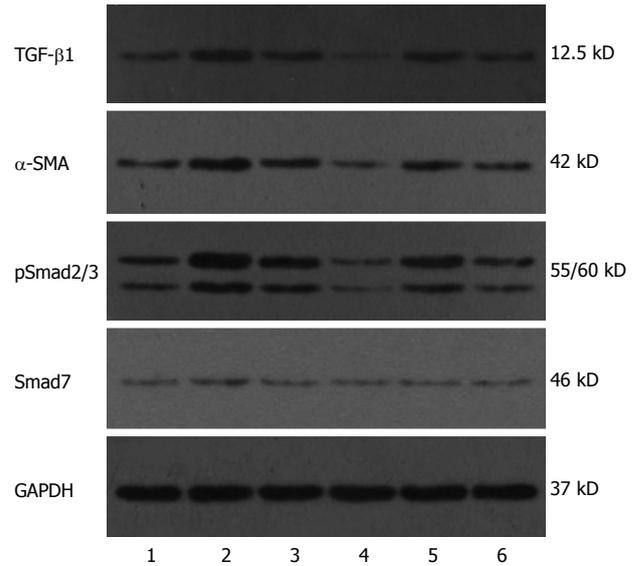
Figure 5 Representative electrophoretic bands of transforming growth factor-beta 1, alpha-smooth muscle actin, pSmad2/3 and Smad7 protein (Western blotting). Numbers 1-3 represent group A, B and C, respectively, at 9 wk. Numbers 4-6 represent group A, B and C, respectively, at 15 wk. The 37 kD glyceraldehyde-3-phosphate dehydrogenase (GAPDH) was used as an internal control. TGF-β1: Transforming growth factor-beta 1; α-SMA: Alpha-smooth muscle actin.
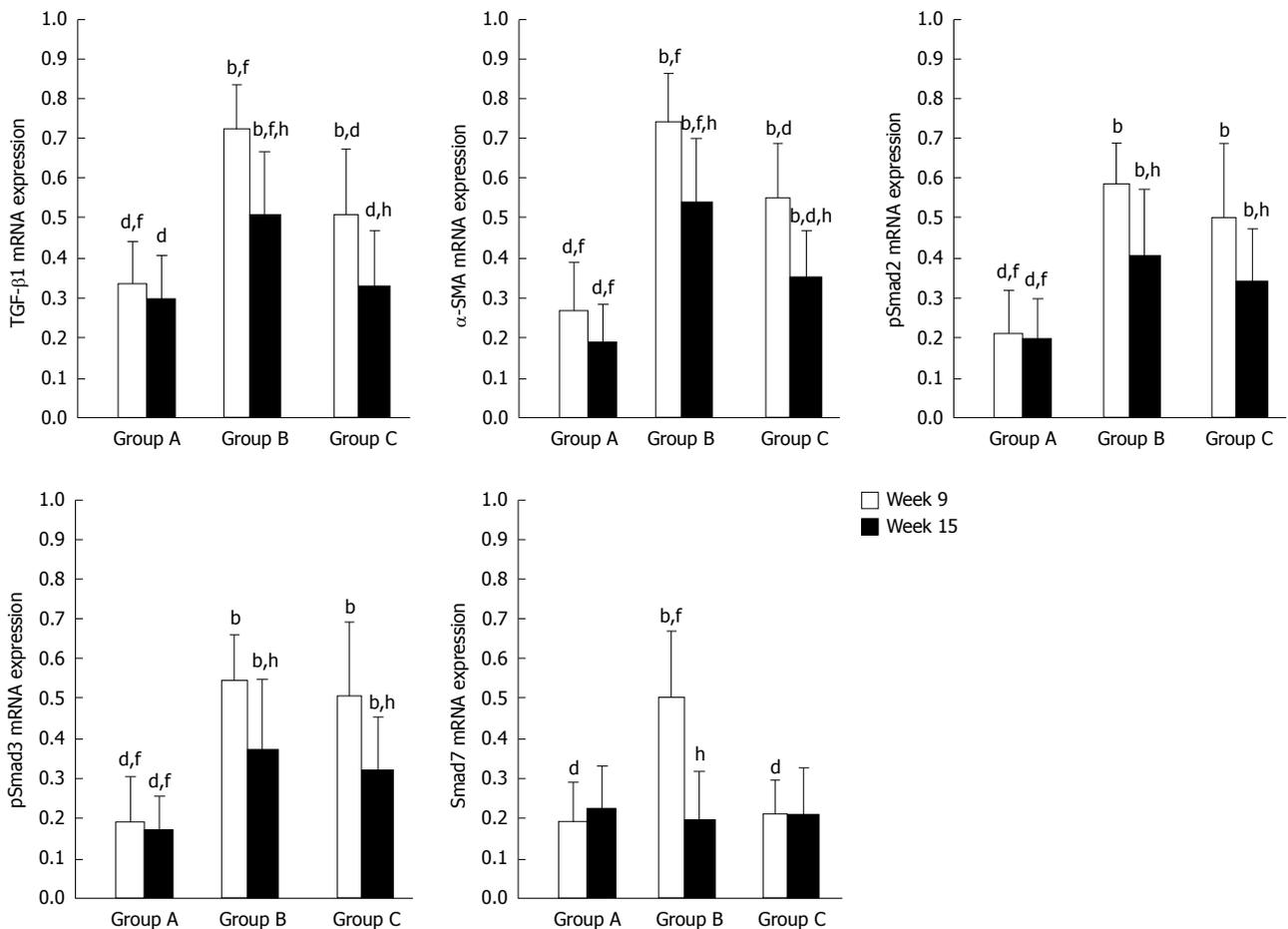
Figure 6 Relative mRNA expressions (target gene integral optical density/glyceraldehyde-3-phosphate dehydrogenase integral optical density, reverse transcription-polymerase chain reaction) of transforming growth factor-beta 1, alpha-smooth muscle actin, pSmad2, pSmad3 and Smad7. TGF-β1: Transforming growth factor-beta 1; α-SMA: Alpha-smooth muscle actin. $^{b}P < 0.01$ *vs* group A; $^{d}P < 0.01$ *vs* group B; $^{f}P < 0.01$ *vs* group C; $^{h}P < 0.01$ *vs* week 9.
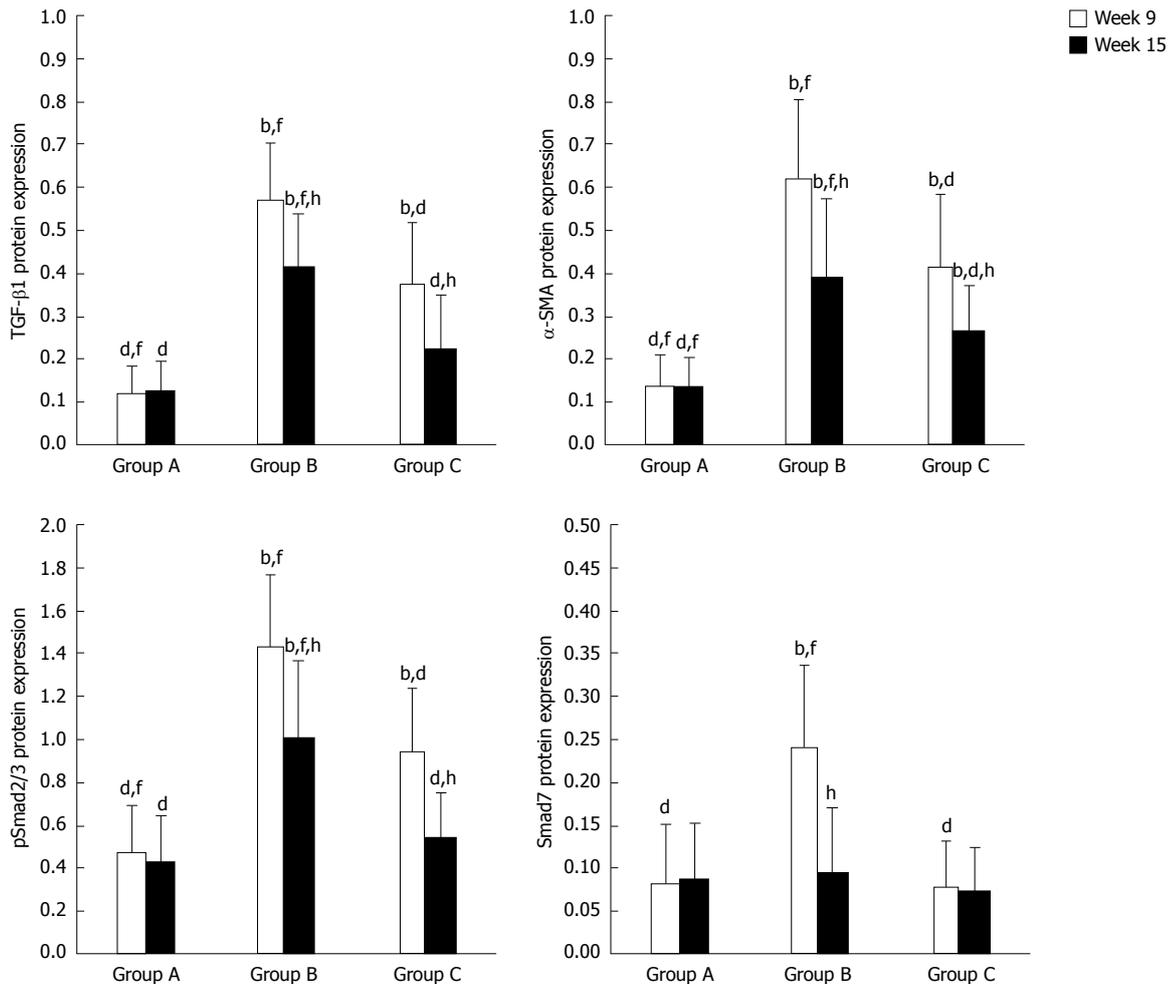
Figure 7 Relative protein expressions (target protein integral optical density/glyceraldehyde-3-phosphate dehydrogenase integral optical density, Western blotting) of transforming growth factor-beta 1, alpha-smooth muscle actin, pSmad2/3 and Smad7. TGF-β1: Transforming growth factor-beta 1; α-SMA: Alpha-smooth muscle actin. [b]$P < 0.01$ *vs* group A; [d]$P < 0.01$ *vs* group B; [f]$P < 0.01$ *vs* group C; [h]$P < 0.01$ *vs* week 9.

the TGF-β superfamily due to their shared morphological characteristics, it has an almost contrary biological function compared to TGF-β. An increasing number of reports indicate that BMP-7 may be a new antagonist of organ fibrosis because of its counteractive effect on the TGF-β/Smad signaling pathway; however, the role of BMP-7 in schistosomal hepatic fibrosis and the underlying regulatory mechanism remains a mystery. The pathogenic progression and prognosis of hepatic fibrosis induced by *S. japonicum* infection are different to other types of hepatic fibrosis, and correlative studies are necessary.

In the present study, we administered recombinant human BMP-7 at the initiation of hepatic schistosomiasis and extended the treatment period to 3 wk to ensure an adequate biological effect. The data showed that both the acute and chronic phases of liver injury and collagen deposition in the model group were accompanied by high expressions of protein and mRNA of TGF-β1, pSmad2/3 and α-SMA compared to the normal group, indicating that the "TGF-β1 active HSCs *via* pSmad2/3" classic pathway is still active in *S. japonicum*-induced hepatic fibrosis. Following treatment with BMP-7, the degree

of collagen deposition significantly reduced at both time points as well as the expressions of TGF-β1, pSmad2/3 and α-SMA, indicating that BMP-7 had an inhibitory effect on schistosomal hepatic fibrosis, at least partly *via* down regulation of the expressions of TGF-β1 and pSmad2/3 and then suppression of HSC activation. Although Smad2 and Smad3 are activated only in response to TGF-β, there are still other Smads through which BMP-7 can promote fibrosis without TGF-β. For instance, Kinoshita found that BMP-7 utilized Smad1/5/8 as signaling intermediates and decreased the expression of type I collagen and α-SMA in primary cultured HSCs independent of the presence of TGF-β[35]. Whether the above cytokines act in schistosomal hepatic fibrosis requires further research.

Smad7, known as a negative feedback regulator to profibrotic TGF-β1, seems only to act in the acute phase of schistosomal liver injury. In this stage, hepatic damage caused by schistosome eggs induces severe inflammation; to prevent further acute injury, reparative fibrosis starts and numerous collagen fibers are secreted. We speculate that the upregulation of Smad7 is decided by the inten-

sity of hepatic fibrosis, that is, only an extremely high degree of TGF-β1 activity and collagen secretion can initiate the negative feedback effect of Smad7. This assumption is based on the following two reasons: firstly, at 15 wk after infection in the model group, hepatic fibrosis was present, but at a lower degree than previously, however, the expression of Smad7 was almost down to normal levels; secondly, after the administration of BMP-7, the degree of hepatic fibrosis at 9 wk after infection was markedly alleviated, accompanied by a lack of Smad7 induction. Interestingly, a previous report on an animal model of CCl4-induced liver fibrosis showed that Smad7 levels (both mRNA and protein) were up-regulated in the model group in a time-dependent manner which lasted 12 wk after modeling compared to the control group, and at week 12 Smad7 was significantly lower in the BMP-7 treatment group than in the model group and control group[36]. Thus, our speculation regarding the expression pattern of BMP-7 remains controversial and needs further verification.

In conclusion, the role of BMP-7 as an antagonist to the TGF-β1/Smads signaling pathway and its antifibrotic effect during both the extreme and stationary phases of schistosomal hepatic fibrosis were confirmed in this study. This provides a new research strategy and offers therapeutic potential in the treatment of hepatic schistosomiasis, although the detailed intervention mechanism still requires more research. In addition, the preparatory work for the clinical application of BMP-7 is a long, arduous task.

COMMENTS

Background
There are currently few effective therapies for schistosomal hepatic fibrosis due to a lack of appropriate intervention targets. Research on antagonists which counteract key pro-fibrosis cytokines or signaling pathways has become a new attractive focus.

Research frontiers
The therapeutic potential of bone morphogenetic protein-7 (BMP-7) as an antagonist target of transforming growth factor-beta (TGF-β)/Smad signaling has been recognized recently based on research on renal fibrosis and thioacetamide/CCl4-induced liver fibrosis. However, its role in schistosomal hepatic fibrosis is still unclear and urgently needs to be explored, as the global epidemic of this disease is becoming more serious.

Innovations and breakthroughs
This study firstly observed the role of BMP-7 as an antagonist to TGF-β1/Smads signaling in schistosomal hepatic fibrosis, and then confirmed the antifibrotic effect of exogenous BMP-7 during both the extreme and stationary phase of this pathological process.

Applications
This study indicates the therapeutic potential of BMP-7 in the treatment of schistosomal hepatic fibrosis and provides a new research strategy related to cytokine regulators.

Peer review
The authors are to be congratulated for confirming that BMP-7 has an inhibitory effect during both the extreme and stationary phase of schistosomal hepatic fibrosis, "at least partly" *via* down regulating the expressions of TGF-β1 and pSmad2/3 then suppressing the activation of hepatic stellate cell. This study provides a new research strategy and offers therapeutically potential for the treatment of hepatic schistosomiasis.

REFERENCES

1   **Zhou XN**, Wang LY, Chen MG, Wu XH, Jiang QW, Chen XY, Zheng J, Utzinger J. The public health significance and control of schistosomiasis in China--then and now. *Acta Trop* 2005; **96**: 97-105 [PMID: 16125655 DOI: 10.1016/j.actatropica.2005.07.005]

2   **McManus DP**, Li Y, Gray DJ, Ross AG. Conquering 'snail fever': schistosomiasis and its control in China. *Expert Rev Anti Infect Ther* 2009; **7**: 473-485 [PMID: 19400766 DOI: 10.1586/eri.09.17]

3   **Zhou XN**, Bergquist R, Leonardo L, Yang GJ, Yang K, Sudomo M, Olveda R. Schistosomiasis japonica control and research needs. *Adv Parasitol* 2010; **72**: 145-178 [PMID: 20624531 DOI: 10.1016/S0065-308X(10)72006-6]

4   **Cheever AW**, Byram JE, von Lichtenberg F. Immunopathology of Schistosoma japonicum infection in athymic mice. *Parasite Immunol* 1985; **7**: 387-398 [PMID: 4034237 DOI: 10.1111/j.1365-3024.1985.tb00085.x]

5   **Hsü SY**, Hsü HF, Davis JR, Lust GL. Comparative studies on the lesions caused by eggs of Schistosoma japonicum and Schistosoma mansoni in livers of albino mice and rhesus monkeys. *Ann Trop Med Parasitol* 1972; **66**: 89-97 [PMID: 4623247]

6   **Hurst MH**, Willingham AL, Lindberg R. Tissue responses in experimental schistosomiasis japonica in the pig: a histopathologic study of different stages of single low- or high-dose infections. *Am J Trop Med Hyg* 2000; **62**: 45-56 [PMID: 10761723]

7   **Hurst MH**, Lola SG, Lindberg R. Immunomodulation of the hepatic egg granuloma in Schistosoma japonicum-infected pigs. *Parasite Immunol* 2006; **28**: 681-686 [PMID: 17096648 DOI: 10.1111/j.1365-3024.2006.00921.x]

8   **Andrade ZA**. Schistosomiasis and liver fibrosis. *Parasite Immunol* 2009; **31**: 656-663 [PMID: 19825105 DOI: 10.1111/j.1365-3024.2009.01157.x]

9   **Inagaki Y**, Okazaki I. Emerging insights into Transforming growth factor beta Smad signal in hepatic fibrogenesis. *Gut* 2007; **56**: 284-292 [PMID: 17303605 DOI: 10.1136/gut.2005.088690]

10 **Brenner DA**. Molecular pathogenesis of liver fibrosis. *Trans Am Clin Climatol Assoc* 2009; **120**: 361-368 [PMID: 19768189]

11 **Senoo H**, Yoshikawa K, Morii M, Miura M, Imai K, Mezaki Y. Hepatic stellate cell (vitamin A-storing cell) and its relative--past, present and future. *Cell Biol Int* 2010; **34**: 1247-1272 [PMID: 21067523 DOI: 10.1042/CBI20100321]

12 **Paiva LA**, Maya-Monteiro CM, Bandeira-Melo C, Silva PM, El-Cheikh MC, Teodoro AJ, Borojevic R, Perez SA, Bozza PT. Interplay of cysteinyl leukotrienes and TGF-β in the activation of hepatic stellate cells from Schistosoma mansoni granulomas. *Biochim Biophys Acta* 2010; **1801**: 1341-1348 [PMID: 20817008 DOI: 10.1016/j.bbalip.2010.08.014]

13 **Anthony B**, Allen JT, Li YS, McManus DP. Hepatic stellate cells and parasite-induced liver fibrosis. *Parasit Vectors* 2010; **3**: 60 [PMID: 20663176 DOI: 10.1186/1756-3305-3-60]

14 **Chapadeiro E**, Pitanga LC. On the reversal of schistosomiasis hepatic fibrosis after specific therapy. Histopathologic study. *Rev Soc Bras Med Trop* 1996; **30**: 53-56 [PMID: 9026832]

15 **Kasinathan RS**, Morgan WM, Greenberg RM. Schistosoma mansoni express higher levels of multidrug resistance-associated protein 1 (SmMRP1) in juvenile worms and in response to praziquantel. *Mol Biochem Parasitol* 2010; **173**: 25-31 [PMID: 20470831 DOI: 10.1016/j.molbiopara.2010.05.003]

16 **Baghy K**, Iozzo RV, Kovalszky I. Decorin-TGFβ axis in hepatic fibrosis and cirrhosis. *J Histochem Cytochem* 2012; **60**: 262-268 [PMID: 22260996 DOI: 10.1369/0022155412438104]

17 **Dooley S**, ten Dijke P. TGF-β in progression of liver disease. *Cell Tissue Res* 2012; **347**: 245-256 [PMID: 22006249 DOI: 10.1007/s00441-011-1246-y]

18   **Wrana JL**. Regulation of Smad activity. *Cell* 2000; **100**: 189-192 [PMID: 10660041]

19   **Shi Y**, Massagué J. Mechanisms of TGF-beta signaling from cell membrane to the nucleus. *Cell* 2003; **113**: 685-700 [PMID: 12809600 DOI: 10.1016/S0092-8674(03)00432-X]

20   **Hayashi H**, Abdollah S, Qiu Y, Cai J, Xu YY, Grinnell BW, Richardson MA, Topper JN, Gimbrone MA, Wrana JL, Falb D. The MAD-related protein Smad7 associates with the TGFbeta receptor and functions as an antagonist of TGFbeta signaling. *Cell* 1997; **89**: 1165-1173 [PMID: 9215638 DOI: 10.1016/S0092-8674(00)80303-7]

21   **Nakao A**, Afrakhte M, Morén A, Nakayama T, Christian JL, Heuchel R, Itoh S, Kawabata M, Heldin NE, Heldin CH, ten Dijke P. Identification of Smad7, a TGFbeta-inducible antagonist of TGF-beta signalling. *Nature* 1997; **389**: 631-635 [PMID: 9335507 DOI: 10.1038/39369]

22   **Kingsley DM**, Bland AE, Grubber JM, Marker PC, Russell LB, Copeland NG, Jenkins NA. The mouse short ear skeletal morphogenesis locus is associated with defects in a bone morphogenetic member of the TGF beta superfamily. *Cell* 1992; **71**: 399-410 [PMID: 1339316 DOI: 10.1016/0092-8674(92)90510-J]

23   **Ripamonti U**, Reddi AH. Tissue engineering, morphogenesis, and regeneration of the periodontal tissues by bone morphogenetic proteins. *Crit Rev Oral Biol Med* 1997; **8**: 154-163 [PMID: 9167090 DOI: 10.1177/10454411970080020401]

24   **Zeisberg M**, Hanai J, Sugimoto H, Mammoto T, Charytan D, Strutz F, Kalluri R. BMP-7 counteracts TGF-beta1-induced epithelial-to-mesenchymal transition and reverses chronic renal injury. *Nat Med* 2003; **9**: 964-968 [PMID: 12808448 DOI: 10.1038/nm888]

25   **Yang T**, Chen SL, Lu XJ, Shen CY, Liu Y, Chen YP. Bone morphogenetic protein 7 suppresses the progression of hepatic fibrosis and regulates the expression of gremlin and transforming growth factor β1. *Mol Med Report* 2012; **6**: 246-252 [PMID: 22552821 DOI: 10.3892/mmr.2012.892]

26   **Chen BL**, Zhang GY, Wang SP, Li Q, Xu MH, Shen YM, Yan L, Gu H, Li J, Huang YL, Mu YB. The combined treatment of praziquantel with osteopontin immunoneutralization reduces liver damage in Schistosoma japonicum-infected mice. *Parasitology* 2012; **139**: 522-529 [PMID: 22309838 DOI: 10.1017/S0031182011002241]

27   **Zi Z**, Chapnick DA, Liu X. Dynamics of TGF-β/Smad signaling. *FEBS Lett* 2012; **586**: 1921-1928 [PMID: 22710166 DOI: 10.1016/j.febslet.2012.03.063]

28   **Lan HY**, Chung AC. Transforming growth factor-β and Smads. *Contrib Nephrol* 2011; **170**: 75-82 [PMID: 21659760 DOI: 10.1159/000324949]

29   **Cohen MM**. TGF beta/Smad signaling system and its pathologic correlates. *Am J Med Genet A* 2003; **116A**: 1-10 [PMID: 12476444 DOI: 10.1002/ajmg.a.10750]

30   **Lan HY**, Chung AC. TGF-β/Smad signaling in kidney disease. *Semin Nephrol* 2012; **32**: 236-243 [PMID: 22835454 DOI: 10.1016/j.semnephrol.2012.04.002]

31   **Yoshida K**, Matsuzaki K. Differential Regulation of TGF-β/Smad Signaling in Hepatic Stellate Cells between Acute and Chronic Liver Injuries. *Front Physiol* 2012; **3**: 53 [PMID: 22457652 DOI: 10.3389/fphys.2012.00053]

32   **Nagarajan RP**, Zhang J, Li W, Chen Y. Regulation of Smad7 promoter by direct association with Smad3 and Smad4. *J Biol Chem* 1999; **274**: 33412-33418 [PMID: 10559222 DOI: 10.1074/jbc.274.47.33412]

33   **von Gersdorff G**, Susztak K, Rezvani F, Bitzer M, Liang D, Böttinger EP. Smad3 and Smad4 mediate transcriptional activation of the human Smad7 promoter by transforming growth factor beta. *J Biol Chem* 2000; **275**: 11320-11326 [PMID: 10753944 DOI: 10.1074/jbc.275.15.11320]

34   **Stroschein SL**, Wang W, Luo K. Cooperative binding of Smad proteins to two adjacent DNA elements in the plasminogen activator inhibitor-1 promoter mediates transforming growth factor beta-induced smad-dependent transcriptional activation. *J Biol Chem* 1999; **274**: 9431-9441 [PMID: 10092624 DOI: 10.1074/jbc.274.14.9431]

35   **Kinoshita K**, Iimuro Y, Otogawa K, Saika S, Inagaki Y, Nakajima Y, Kawada N, Fujimoto J, Friedman SL, Ikeda K. Adenovirus-mediated expression of BMP-7 suppresses the development of liver fibrosis in rats. *Gut* 2007; **56**: 706-714 [PMID: 17127702 DOI: 10.1136/gut.2006.092460]

36   **Shen CY**, Chen YP, Yang T, Lu XJ, Li CY, Lin Z, Song M. Effects of bone morphogenetic protein-7 therapy on E3 ubiquitin ligase expression in mouse liver with experimentally induced fibrosis. *Zhonghua Ganzangbing Zazhi* 2012; **20**: 671-676 [PMID: 23207231 DOI: 10.3760/cma.j.issn.1007-3418.2012.09.007]